Anal. Bioanal. Electrochem., Vol. 3, No. 3, 2011, 233-248

Analytical & Bioanalytical Electrochemistry

Full Paper

Three-Dimensionally Microporous Polypyrrole Film as an Efficient Matrix for Enzyme Immobilization

Jing Qian[1], Lei Peng[2], Ulla Wollenberger[2], Frieder W. Scheller[2] and Songqin Liu[1,*]

[1]School of Chemistry and Chemical Engineering, Southeast University, Nanjing, 211189, P. R. China

[2]Department of Analytical Biochemistry, Institute of Biochemistry and Biology, University of Potsdam, Karl-Liebknecht-Strasse 24-25, 14476 Potsdam, Germany

*Corresponding author, Tel: +86-25-52090613; Fax: +86-25-52090618

E-Mail: liusq@seu.edu.cn

Received: 27 January 2011/ Accepted: 7 June 2011 / Published online: 20 June 2011

Abstract- The development of new porous materials has opened unprecedented opportunities for a wide range of applications. In the present work, a three-dimensionally interconnected porous polypyrrole structure was proposed for biosensing. Silica nanoparticles with good monodispersion and uniformity of the spheres synthesized by improved Stöber methods was used as template for porous polypyrrole electrodeposition. Voltammetric and electrochemical impedance measurements showed that the polypyrrole 3D-network arrays provided excellent matrices for the immobilization of horseradish peroxidase. The immobilized horseradish peroxidase on these polypyrrole 3D-network arrays retained its bioactivity effectively and displayed a pair of redox peaks with a formal potential of -0.275 V and an excellent electrocatalytic response toward the reduction of hydrogen peroxide (H_2O_2). This allowed the detection of H_2O_2 concentration with a linear range from 1 μM to 7.94 μM. The detection limit was found to be 0.22 μM at a signal-to-noise ratio of 3. This method provided an alternative way for the biosensor construction.

Keywords- Silica Template, 3D-Network Arrays, Horseradish Peroxidase, Porous Polypyrrole

1. INTRODUCTION

Current studies on the direct electron transfer between immobilized redox-proteins and electrode surface has received wide attention due to their distinguished applications in biological science, environmental science, energy science and analytical chemistry [1-3]. Early reports demonstrated that the redox protein immobilized on a biocompatible electrode surface exhibited enhanced electrochemical activity, which allowed the electrochemical measurement of its substrate with higher sensitivity and better selectivity [4,5]. The most popular materials for protein immobilization are polyacrylamide hydrogel [6] surfactant [7,8] DNA [9] and a series of nanostructured materials such as calcium phosphate,10 colloidal gold [11,12] clay [13] ZnO [14] grapheme [15,16] TiO_2 [17] and carbon nanotubes [18,19]. These materials facilitated direct chemically reversible electron exchange between redox proteins and electrodes, and are thus being widely used in sensor construction .

The development of new porous materials has opened unprecedented opportunities for a wide range of applications [20,21] Several chemical preparations of ordered micro- and macroporous materials based on colloidal crystal templates have been described [22-30]. These methods use close-packed arrays of monodisperse spheres as templates for the formation of three-dimensionally ordered micro- or macroporous structures in a range of materials, such as silica [22,23] metals [24,25] carbon [26,27] and polymers [28-30]. One of the characteristics of porous materials is their high surface-area/volume ratio, favoring thereby the interaction with external reagents[31] which could allow immobilization of suitable proteins likely to induce novel properties and pave the way to be exploited in biosensing applications [32,33]. For example, a three-dimensional (3D) porous chitosan membrane material prepared by electrodeposition of chitosan-encapsulated silica nanoparticle on an ITO electrode, followed by removal of silica nanoparticles with HF solution, was used as a matrix for hepatitis B surface antibody immobilization. It was shown that the 3D chitosan porous structure possesses high surface area, good mechanical stability, good biocompatibility and increased protein loading. These benefits allowed the resultant immunosensor to have a wide linear range and low detection limit [34]. With calcium carbonate microsphere as carrier for the loading of cadmium telluride quantum dots, Zhu and co-workers [35] developed a protein-CdTe-$CaCO_3$@polyelectrolyte 3D architecture for electrochemistry biosensing. The unique properties of $CaCO_3$, such as good biocampatibility and its channel-like structure, allowed the formation of a thick and uniform quantum-dot ‘‘shell’’, which in turn improved the soluble stability of the spheres and contributed to a fast and effective direct electron transfer between the protein redox center and the macroscopic electrode.

The present work was also motivated by the very promising applications of 3D structure materials in protein immobilization for electrochemical biosensing. In order to achieve the 3D porous interconnected polypyrrole structure, silica nanoparticles with good

monodispersion and uniformity of spheres, synthesized by improved Stöber methods[36] were chosen as templates. The porous polypyrrole film on the gold electrode surface provided excellent matrices for the immobilization of horseradish peroxidase (HRP). The immobilized HRP not only retained its bioactivity but also showed a high affinity for H_2O_2 reduction, which produced a novel H_2O_2 biosensor.

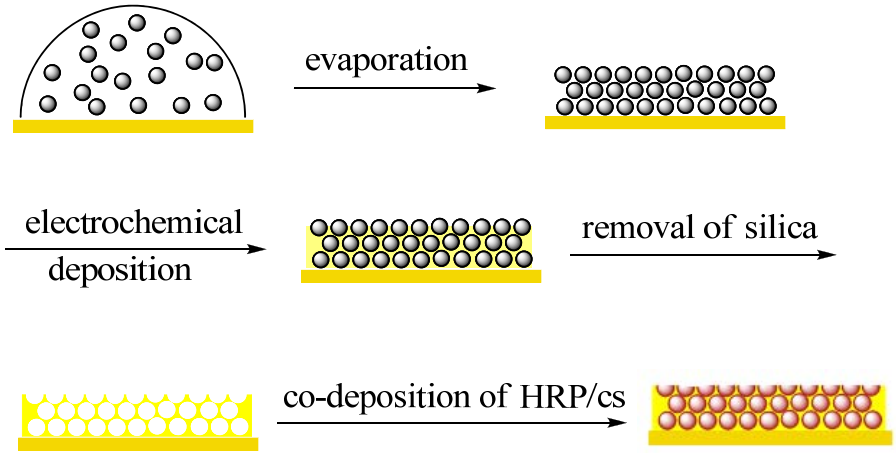

Scheme 1. Schematic representation of the fabrication procedure for 3D porous- Ppy/Au and HRP immobilization

2. MATERIALS AND METHODS

2.1. Materials

Horseradish peroxidase (HRP, EC 1.11.1.7, RZ 3.2, 290 purpurogallin units per mg solid, from horseradish), chitosan (CS, from crab shells, minimum 85% deacetylated), and pyrrole were obtained from Sigmaaldrich. 0.1 M pH 7.0 phosphate buffer solution (PBS) was prepared by mixture of NaH_2PO_4 and Na_2HPO_4 stock solution, and was modulated by H_3PO_4 and NaOH. 10 mg/mL HRP was prepared by 0.1 M pH 7.0 PBS, 1% CS solution was prepared by 1% acetic acid. All other chemicals were analytical grade reagents. All the solutions were prepared with doubly distilled water and stored in a refrigerator at 4 ^oC when not in use.

2.2. Apparatus

Cyclic voltammetry(CV) and amperometric measurement were conducted with a three-electrode system comprised of the modified gold electrodes as a working electrode, an Ag/AgCl (1 M KCl) as reference electrode, and a platinum wire auxiliary electrode. The electrodes were connected to a computer-controlled CHI750A electrochemical analyzer. All electrochemical experiments were carried out in 1 mL of 0.1 mol L^{-1} phosphate buffer (pH 7.0, apart from the pH parameter experiments) at room temperature. H_2O_2 was added to

PBS while being stirred. All experimental solutions were thoroughly deoxygenated by bubbling nitrogen through the solution for at least 10 min .

Electrochemical impedance spectroscopy (EIS) was performed with Gamery Instruments (Reference 600, USA) in 5 mM $[Fe(CN)_6]^{3-/4-}$ mixture with 0.1 M KCl as supporting electrolyte. An alternating current voltage of 5.0 mV was used, within the frequency range of 0.1-100 kHz .

2.3. Preparation of the 3D Ppy modified Electrode

The monodispersed SiO_2 spheres with diameters of 180±3 nm were synthesized with an improved Stöber seed-growth method, which we previous reported [36]. The silica nanosphere templates were built by dispersing of a dilute suspension of SiO_2 nanospheres onto a gold disc electrode surface. In this case, the gold disc electrode was polished before each experiment with 1.0, 0.3 and 0.05 μm alumina powder, respectively, and followed by a thorough wash with acetone and doubly distilled water. Au electrode was dipped into dilute silica suspension in ethanol for 10 s, and then Au electrode was put out and allowed to evaporate the solvent naturally. After that, the resultant Au electrode was dipped into a 0.1 M KCl solution (adjust pH to 2.0 with HCl) that contained 0.05 M pyrrole for 2 min. Polypyrrole was deposited into the void spaces of such a template through CV, at the potential window of 0 to 0.7 V (*vs*. Ag/AgCl). After deposition, the silica template was etched by aqueous HF (5%) for about 5 min to leave behind an ordered porous polypyrrole framework, donated as porous-Ppy/Au. Finally, the electrode was immersed in PBS for at least 30 min for the following use .

2.4. Immobilization of HRP

The immobilization of HRP on porous-Ppy/Au was performed through an electrochemical co-deposition process. The Ppy/Au was dipped in a HRP/CS solution at -2.5 V for 300 s. HRP/CS solution was prepared by a mixture that involved equal volumes of 10 mg/mL HRP solution in 0.1 M pH 7.0 PBS and 1% CS solution in 1% acetic acid (1:1, v/v). After deposition the electrode was removed and rinsed with water to obtain a HRP/CS modified electrode (HRP/CS-porous-Ppy/Au). In contrast, CS- porous-Ppy/Au, the porous-Ppy/Au deposited in CS solution in the absence of HRP, were used for control measurements.

3. RESULTS AND DISCUSSION

3.1. The synthesis of the porous-Ppy/Au

The porous-Ppy/Au was prepared based on the silica nanosphere template. The responses of the electrochemical probe to the resultant porous-Ppy film were checked by CV, as shown in Fig. 1. When the Ppy was electrodeposited into the void spaces of the template, the resultant silica-Ppy/Au (Fig. 1, curve b) displayed much lower signals in a $[Fe(CN)_6]^{3-/4-}$

containing solution than that of the bare gold electrode (Fig. 1, curve a). This indicated the formation of silica nanospheres doped Ppy layer on the electrode surface, which can effectively block electron transfer between the electroactive species and electrode. This would have produced a poor electrochemical response [37]. After the removal of silica nanosphere templates with 5% HF solution, the porous-Ppy/Au (Fig. 1, curve c) displayed a large response to the $[Fe(CN)_6]^{3-}$ probe. Both the anode and anode peak current were much larger than that of silica nanospheres doped Ppy film, but still smaller than that of the bare electrode. This observation suggested the formation of the porous Ppy film on the electrode surface, which partly hindered the electron transfer between $[Fe(CN)_6]^{3-/4-}$ species and the electrode .

In addition, the anode and anode peak current of the silica-Ppy/Au decreased with an increase of the deposition cycles from 3 to 9, which related to the amount of Ppy coated onto silica template (data not shown). When the pyrrole was deposited on the Au electrode for 9 cycles, both the peak currents of silica-Ppy/Au reached a minimum value (Fig. 1, curve c). This low value indicated the formation of a dense Ppy film on gold electrode, which effectively blocked the electron transfer between $[Fe(CN)_6]^{3-/4-}$ species and the electrode. The CV of silica-Ppy/Au has the same shape as the ones deposited for 9 and 12 cycles. Despite this, no changes were observed after the removal of silica template with aqueous HF for 12 cycles, which suggested that the Ppy film was too thick for HF to efficiently remove from porous polypyrrole framework on gold. Therefore, the pyrrole deposited for 9 cycles was selected in the following study.

The formation of the porous Ppy film, after being removed from the silica template, was illustrated by the re-coupling tests. When the porous-Ppy/Au was again soaked in a silica nanosphere suspension for 10 s, the Au electrode was also put out and evaporation of the solvent was allowed. The electrode displayed similar response to silica-Ppy/Au (Fig. 1, curve b and d), which indicated the re-coupling of silica nanospheres into the pore of the porous-Ppy/Au. The slight decrease of the electrochemical response to $[Fe(CN)_6]$3-/4- for silica nanospheres re-coupled electrode compared to that of silica-Ppy/Au suggested the re-coupling process allowed more silica nanoparticles to be attached on the electrode. Some silica nanoparticles were able to attach in the hole and some was covered on the surface.

The formation of the porous Ppy film, after being removed from the silica template, was also supported by the electrochemical impedance spectra. The impedance measurements were carried out in 0.1 M KCl that contained 5 mM $[Fe(CN)_6]^{3-/4-}$ and at open circuit potential. Fig.2 presents the Nyquist plots of the different electrodes. After deposition of Ppy for 9 cycles, the charge-transfer resistance (Rct) of the bare gold electrode (Fig. 2, curve a) was much smaller than that of the silica-Ppy/Au (Fig. 2, curve b). The increase of impedance from 212.5 Ω to 2275.6 Ω of the silica-Ppy/Au relatve to the bare gold electrode was due to the formation of Ppy film on gold surface. The coat of Ppy blocked the diffusion of redox species

to the electrode surface, which made the redox process more difficult and caused the impedance to increase. After immersion of the silica-Ppy/Au in HF solution for 5 min, the impedance decreased from 2275.6 Ω to 891.2 Ω due to the release of silica nanospheres from the silica-Ppy film. However, the impedance was still greater than that of bare gold electrode, which indicated that the retention of Ppy film on the gold surface. After a second immersion of this electrode in a silica suspension for 10 s, the impedance (Fig. 2, curve d) began to increase from 891.2 Ω to 2860.5 Ω. This was slightly larger than in Fig. 2, curve b, which indicated the presence of re-coupled silica nanospheres on the Ppy film. Repeated experiments produced very similar results. These results indicated the formation of porous Ppy film on gold and that the changes in impedance were due to the reversible coupling and release of silica nanospheres.

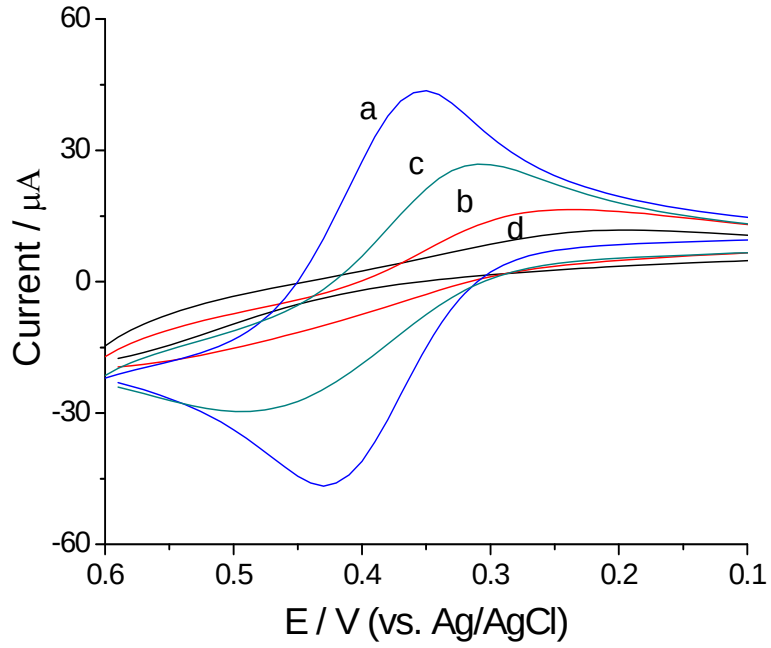

Fig. 1. The cyclic voltammograms of (a) bare Au, (b) silica-Ppy/Au, (c) porous- Ppy/Au, and (d) re-coupled silica on porous-Ppy/Au in 0.1 M KCl that contained 5.0 mM $[Fe(CN)_6]^{3-/4-}$ at 100 mVs^{-1}. The Ppy was electrodeposited in a 0.1 M pH 2.0 KCl+HCl+0.05 M pyrrole solution through 9 cycles of CV

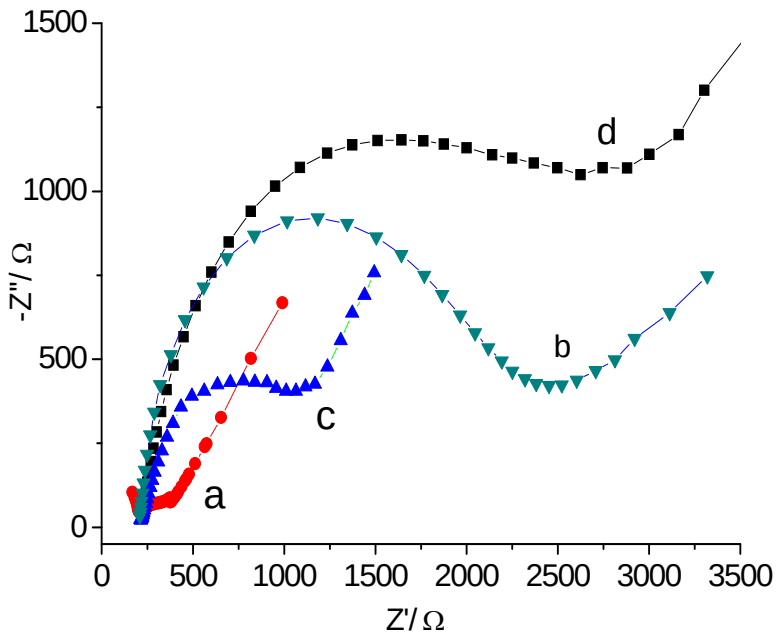

Fig. 2. EIS of (a) bare Au, (b) silica-Ppy/Au, (c) porous-Ppy/Au, and (d) re-coupling of silica nanoparticles on porous-Ppy/Au in 0.1 M KCl that contained 5.0 mM $[Fe(CN)_6]^{3-/4-}$

3.2. Direct Electrochemistry of immobilized HRP on porous-Ppy/Au

The immobilization of HRP on porous-Ppy/Au was performed through an electrochemical co-deposition process; the Ppy/Au was dipped in a HRP/CS solution at -2.5 V for 300 s. At the applied potential of -2.5 V, the H^+ in HRP/CS colloidal solution could be reduced to H_2, which would result in a gradual increase in pH value at the electrode surface. Since the solubility of CS is pH dependent, when the pH was higher than the pK_a of CS (about 6.3), the dissolved CS would flocculate to form an insoluble hydrogel network due to deprotonation of its amine groups. As a result, CS hydrogel incorporated with HRP was electrodeposited on the cathode surface.

The co-immobilization of HRP with CS on porous-Ppy/Au could be demonstrated by comparison of the impedance of HRP/CS-porous-Ppy/Au with CS-porous-Ppy/Au, as shown in Fig. 3A. The impedance of HRP/CS-porous-Ppy/Au was much larger than that of CS-porous-Ppy/Au. The increase of impedance from 675.3 Ω to 3611.5 Ω indicated the incorporation of the insulation of the protein shell into CS film.

The HRP/CS-porous-Ppy/Au was characterized by CV. Fig. 3B showed the typical CVs obtained from porous-Ppy/Au (Fig. 3B, curve a), HRP/CS/Au (Fig. 3B, curve b), and HRP-porous-Ppy/Au (Fig. 3B, curve c) in 0.1 M pH 7.0 PBS at 100 mV s^{-1}, respectively. HRP-porous-Ppy/Au exhibited a cathodic peak at -312.5 mV, with the corresponding anodic peak on the reverse scan, at -238.2 mV. No peak was observed at either bare gold or porous-

Ppy/Au, which suggested that the response of HRP-porous-Ppy/Au is attributed to the redox of the electroactive center of HRP on electrode surface [39].

The surface concentration of electroactive HRP (Γ*) for porous-Ppy film was deduced from the following equation [40]:

$$\Gamma^* = Q/nFA$$

Where Q is the charge, the electron transfer number is n = 1, F is the Faraday constant, and A denotes the effective surface area of the working electrode. From the integration of the anodic peak of the sensor, the surface concentration of the active HRP on HRP/CS-porous-Ppy/Au surfaces were calculated to be 2.80×10^{-10} mol cm^{-2}. The HRP/CS-porous-Ppy/Au collected a higher concentration of the electroactive HRP, which was about 6 times the monolayer coverage of HRP (5.0×10^{-11} mol cm^{-2}) on 3-mercapto-propionic acid modified gold electrode [41]. This suggested that multiple layers of HRP were coated on the electrode. Comparing this calculated value with those reported for HRP surface concentration in other immobilized matrices, such as DNA (5.1×10^{-11} mol cm^{-2}),42 2.466×10^{-10} mol cm^{-2} for multilayer of HRP on ZnO nanorods.43 Porous-Ppy matrix was more efficient for HRP immobilization.

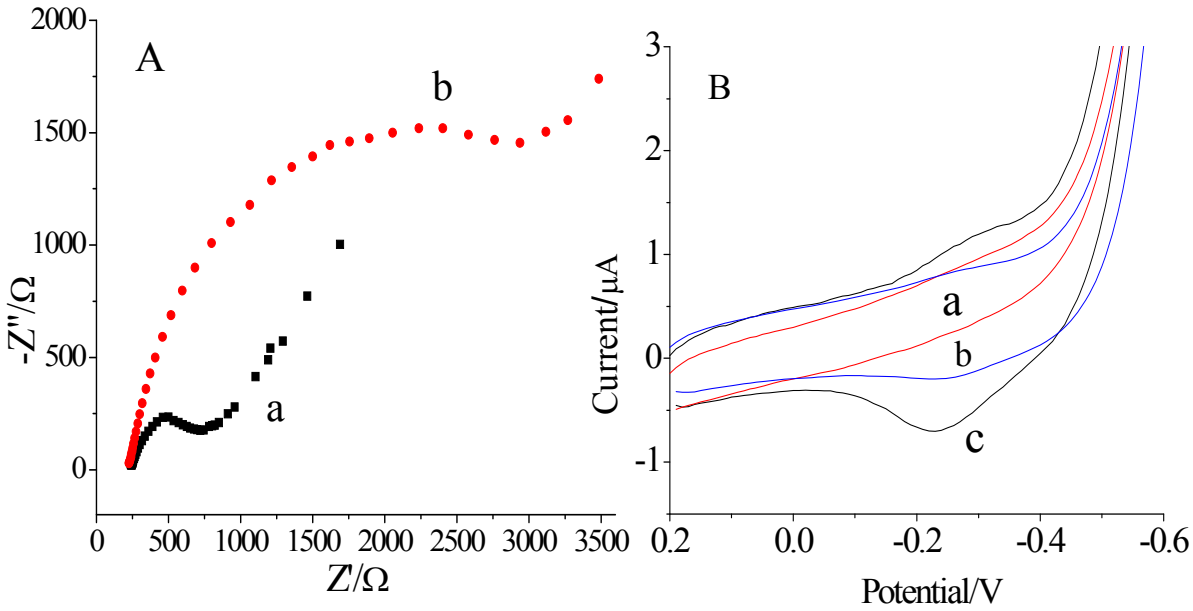

Fig. 3. EIS (A) of CS-p-Ppy/Au (a) and HRP/CS-porous-Ppy/Au (b) in 0.1 M, KCl that contained 5.0 mM $[Fe(CN)6]^{3-/4-}$, and CVs (B) of porous-Ppy/Au (a), HRP/cs/Au (b), and HRP/CS-porous-Ppy/Au(c) in 0.1 M, PBS (pH 7.0) with scan rate 100 mV s^{-1}

As shown in Fig. 4, the cathodic and anodic peak current (I_{pc}) increased gradually when the scan rate was accelerated from 10 to 1000 mV s^{-1}. Insert of Fig. 4 plotted the I_{pc} versus the scan rate and revealed their linear relationship. This indicated that the redox reaction is a surface process and the electrons easily transfer between HRP and porous-Ppy/Au electrode [43]. It proved that the HRP was successfully immobilized on the porous-Ppy/Au and that it retained its bioactivity perfectly. The kinetics of the direct electron transfer was analyzed using the model of Laviron. Suppose that the charge transfer coefficient, α, is between 0.3 and 0.7, the electron transfer rates, ks, can be estimated with the formula k_s=mnFv/RT when the peak-to-peak separation is less than 200 mV [44] where m is a parameter related to the peak-to-peak separation. The peak-to-peak separations of 74.3 mV at 100 mV s^{-1} produced the k_s value of 1.49 s^{-1}, which is close to the reported value from some better biosensors constructed by carbon nanotubes [45]. This value was larger than that obtained at HRP–Au–SPCE (0.75±0.04 s^{-1}) [46] HRP/DNA/PG electrode (1.13 s-1) [47] and close to that obtained at ZnO-GNPs-Nafion-HRP/GCE (1.94 s^{-1}) [48] suggesting the HRP immobilized on porous-Ppy film has perfect catalytic activity, and that the electrons could easily transfer from HRP to electrode. Ppy and chitosan composite film is an effective biocompatible material to retain the bioactivity of HRP.

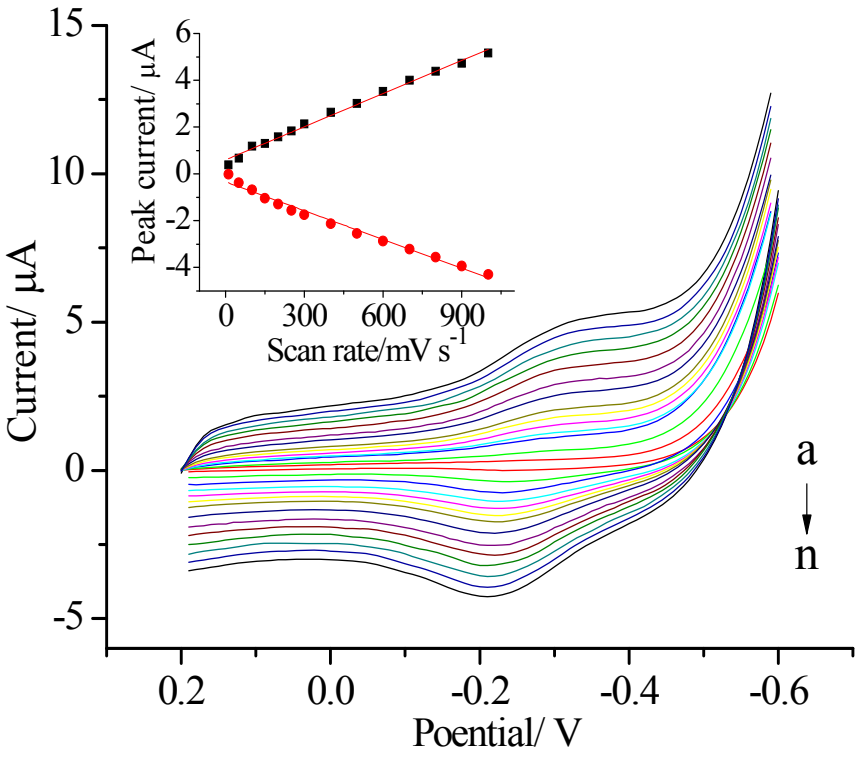

Fig. 4. Cyclic voltammograms of HRP/CS-porous-Ppy/Au at several scan rates: (from a to n: 10, 50, 100, 150, 200, 250, 300, 400, 500, 600, 700, 800, 900, and 1000 mVs^{-1}). Insert is the relationship between peaks current and scan rates

3.3. Response of the HRP/CS-porous-Ppy/Au to H_2O_2

Upon addition of H_2O_2 to PBS, the shape of cyclic voltammogram of HRP-porous-Ppy/Au for direct electron transfer of HRP changed dramatically with an increase of reduction current (Fig. 5). Meanwhile, no obvious change was observed at bare gold and porous-Ppy/Au (date not shown). The increased reduction peak and the decreased oxidation peak current of HRP at HRP-porous-Ppy/Au displayed the obvious electrocatalytic behavior of immobilized HRP to the reduction of H_2O_2. It demonstrated that the HRP immobilized on the porous-Ppy/Au could maintain its activity and catalyzed H_2O_2 reduction effectively.

Fig. 6 illustrated the chronoamperometric response of porous-Ppy/Au (curve a), HRP/CS-porous-Ppy(n=6)/Au (curve b), and HRP/CS-porous-Ppy(n=9)/Au(curve c) with successive additions of H_2O_2 to 0.1 M pH 7.0 PBS. Upon addition, the sensor achieved 95% of the steady-state current in 5 s. The linear response range of the HRP/CS-porous-Ppy(n=9)/Au to H_2O_2 concentration is from 1 μM to 7.94 mM with a correlation coefficient of 0.9982 and a detection limit of 2.2×10^{-7} M, at a signal- to-noise ratio of 3. While the linear response range of the HRP/CS-porous-Ppy (n=6) /Au to H_2O_2 concentration is from 1 μM to 5.77 mM, with a correlation coefficient of 0.9939 and a detection limit of 6.42×10^{-7} M at a signal- to-noise ratio of 3.

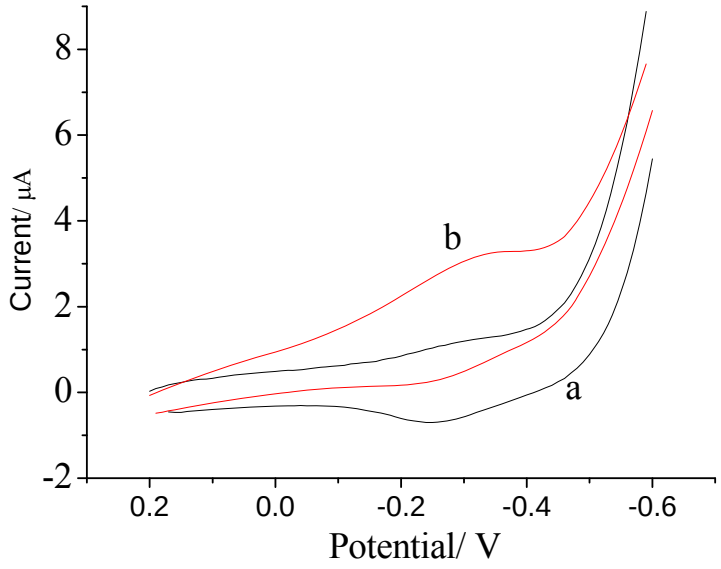

Fig. 5. Cyclic voltammograms of the HRP/CS-porous-Ppy/Au in the absence (a), and presence of 9.90×10^{-5}M (b) H_2O_2

When the concentration of H_2O_2 is higher than 7.94 mM, a platform was observed, which displayed a characteristic of the Michaelis–Menten kinetic mechanism. The apparent Michaelis–Menten constant (K^a_{ppm}), a reflection of both the enzymatic affinity and the ratio

of microscopic kinetic constants, could be obtained from the electrochemical version of the Lineweaver–Burk equation[49]:

$$1/I_{ss}=1/I_{max}+K^{a}_{ppm}/I_{max}C$$

Here I_{ss}, I_{max} and C represented the steady current, maximum current and H_2O_2 concentration, respectively. It is well known that a smaller Kappm implied a higher catalytic activity of the immobilized enzyme.

Based on the Lineweaver-Burk equation, the K^{a}_{ppm} of HRP/CS-porous-Ppy(n=6) and HRP/CS-porous-Ppy(n=9) were calculated to be 58.6 μM and 29.4 μM, respectively. This results was close to the reported value of some better biosensors constructed from silica-hydroxyapatite (HAp) hybrid film-modified glassy carbon electrode (silica/HRP-HAp/GCE) [39].This value was much lower than 0.159 mM for C_{16}-C_{12}-C_{16}-OMIMPF$_6$-HRP/GCE,50 and 1.8 mM for native HRP in solution [51].

As is well-known, the lower apparent Kappm reflected the better affinity effect of enzyme to catalyze target, thus, the result demonstrated that the as immobilized HRP had the maximal catalysis to H_2O_2 reaction.

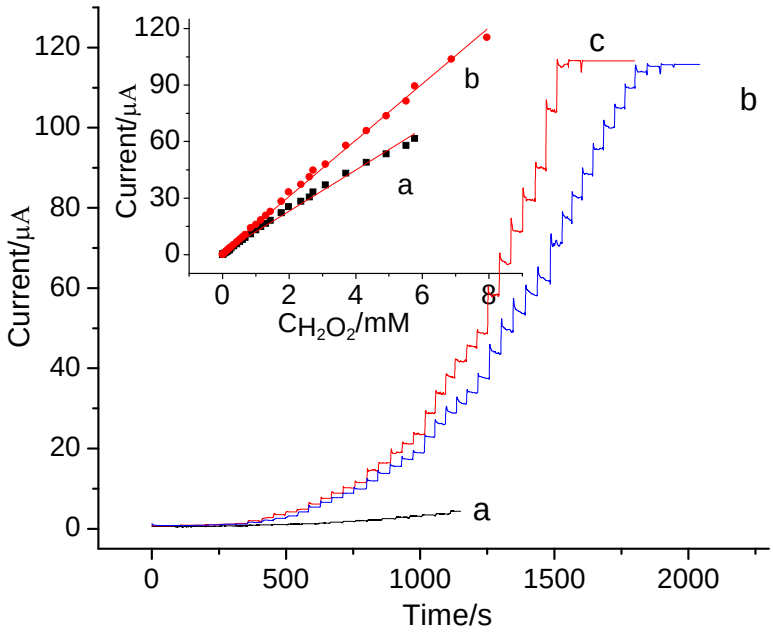

Fig. 6. Typical steady-state response of porous-Ppy/Au(a), HRP/CS-porous-Ppy

3.4. Reproducibility and stability of the biosensor

The measurement repeatability of the HRP/CS-porous-Ppy (n=9)/Au electrode was investigated in 0.1 M PBS with the same electrode. The relative standard deviations (RSD) were 6.5% for 6 successive assays in the presence of 0.1 mM H_2O_2. The fabrication

reproducibility for three HRP electrodes gave a RSD of 5.1% for typical steady-state response at 0.1 mM H_2O_2. The good reproducibility may be due to the fact that the 3D structure was consistent and HRP molecules were attached firmly onto the pores of polypyrrole. The stability of the HRP/CS-porous-Ppy (n=9)/Au was investigated when the current response of 0.1 mM H_2O_2 was measured every 3 days. The results showed that the cathodic peak current only decreased about 8.7% after storage at 4^{o}C in PBS for 2 weeks. Good long-term stability could be attributed to the strong interaction between HRP and chitosan embedded in the polypyrrole network, which prevented the loss of enzymes. Porous polypyrrole-chitosan composite matrix could have provided a biocompatible microenvironment which acted to prevent the desorption of enzyme.

4. CONCLUSIONS

We have developed an innovative method for the preparation of an enzyme biosensor for H_2O_2, through 3D interconnected structures of porous polypyrrole film for the immobilization of HRP, to fabricate a new third-generation H_2O_2 biosensor. The large surface area of the electrodes could be potentially exploited to increase the amount of enzyme molecules loaded on the electrode surface, through the formation of multiple coverage of HRP, via the 3D network. The porous polypyrrole film effectively maintained the bioactivity of HRP. The direct electron transfer between HRP and electrode surface was also achieved. Furthermore, the resultant HRP-porous-Ppy/Au electrode showed electrochemical activity in the reduction of H_2O_2 without the aid of any electron mediator. The proposed biosensor exhibited fast amperometric response, wide linear range, and high sensitivity and stability.

Acknowledgments

We thank the support from DAAD supported project PPP VR China, the National Natural Science Foundation of China (Grant Nos. 20675013, 20875013), the Specialized Research Funds for the Doctoral Program of Higher Education (200802860035).

REFERENCES

[1] X. D. Zeng, X. F. Li, X. Y. Liu, Y. Liu, S. L. Luo, B. Kong, S. L. Yang, and W. Z. Wei, Biosens. Bioelectron. 25 (2009) 896.

[2] T. F. Paulo, I. C. N. Diógenes, and H. D. Abruña. Langmuir 2011, In press, DOI: 10.1021/la103505x.

[3] N. J. Yang, R. Hoffmann, W. Smirnov, A. Kriele, and C. E. Nebel, Electrochem. Commun. 12 (2010) 1218.

[4] Z. J. Wang, M. Y. Li, P. P. Su, Y. J. Zhang, Y. F. Shen, D. X. Han, A. Ivaska, and L. Niu, Electrochem. Commun. 10 (2008) 306.
[5] J. S. Long, D. S. Silvester , G. G. Wildgoose , A. E. Surkus, G. U. Flechsig , and R. G. Compton, Bioelectrochemistry 74 (2008) 183.
[6] X. D. Zeng, W. Z. Wei, X. F. Li, J. X. Zeng, and L. Wu, Bioelectrochemistry 71 (2007) 135.
[7] S. Y. Rhieu, D. R. Ludwig, V. S. Siu, and G. T. R. Palmore, Electrochem. Commun. 11 (2009) 1857.
[8] J. Rajbongshi, D. K. Das, and S. Mazumdar, Electrochim. Acta 55 (2010) 4174.
[9] A. A. Gorodetsky, A. K. Boal, and J. K. Barton, J. Am. Chem. Soc. 128 (2006) 1208.
[10] H. Zhang, J. J. Xu, and H. Y. Chen, J. Electroanal. Chem. 79 (2008) 624.
[11] W. T. Xie, L. L. Kong, M. X. Kan, D. M. Han, X. J. Wang, and H. M. Zhang, J. Nanosci. Nanotechnol. 10 (2010) 6720.
[12] M. A. Rahman, H. B. Noh, and Y. B. Shim, Anal. Chem. 80 (2008) 8020.
[13] K. Charradi, C. Forano, V. Prevot, A. B. H. Amara, and C. Mousty, Langmuir 25, (2009) 10376.
[14] W. Sun, Z. Q. Zhai, D. D. Wang, S. F. Liu, and K. Jiao, Bioelectrochemistry 74 (2009) 295.
[15] C. S. Shan, H. F. Yang, J. F. Song, D. X. Han, A. Ivaska, and L. Niu, Anal. Chem. 81 (2009) 2378.
[16] H. F. Xu, H. Dai, and G. N. Chen, Talanta 81 (2010) 334.
[17] M. C. Liu, G. H. Zhao, K. J. Zhao, X. L. Tong, and Y. T. Tang, Electrochem. Commun. 11 (2009) 1397.
[18] F. H. Li, J. X. Song, F. Li, X. D. Wang, Q. X. Zhang, D. X. Hana, A. Ivaska, and L. Niu, Biosens. Bioelectron. 25 (2009) 883.
[19] P. A. Prakash, U. Yogeswaran, and S. M. Chen, Talanta 78 (2009) 1414.
[20] P. Kuhn, A. L. Forget, D. S. Su, A. Thomas, and M. Antonietti, J. Am. Chem. Soc. 130 (2008) 13333.
[21] J. T. Cheng, Y. Zhang, P. Gopalakrishnakone, and N. G. Chen, Langmuir 25 (2009) 51.
[22] F. Li, Z. Y. Wang, and A. Stein, Chem. Int. Ed. 46 (2007) 1885.
[23] P. L. Falcaro, O. L. Malfatti, T. Kidchob, G. Giannini, A. Falqui, M. F. Casula, H. Amenitsch, B. Marmiroli, G. Grenci, and P. Innocenzi, Chem. Mater. 21 (2009) 2055.
[24] P. N. Bartlett, J. J. Baumberg, P. R. Birkin, M. A. Ghanem, and M. C. Netti, Chem. Mater. 14 (2002) 2199.
[25] V. Urbanová, K. Vytřas, and A. Kuhn, Electrochem. Commun. 12 (2010) 114.
[26] K. P. Gierszal and M. Jaroniec, J. Am. Chem. Soc. 128 (2006) 10026.
[27] S. L. Zhang, L. Chen, S. X. Zhou, D. Y. Zhao, and L. M. Wu, Chem. Mater. 22 (2010) 3433.

[28] J. Li and Y. Zhang, Chem. Mater. 19 (2007) 2581.
[29] J. T. Cheng, Y. Zhang, P. Gopalakrishnakone, and N. G. Chen, Langmuir 25 (2009) 51.
[30] S. L. Zhang, S. X. Zhou, B. You, and L. M. Wu, Macromolecules 42 (2009) 3591.
[31] A. Walcarius and A. Kuhn, TrAC-Trend. Anal. Chem. 27 (2008) 593.
[32] H. Zheng, H. G. Xue, Y. F. Zhang, and Z. Q. Shen, Biosens. Bioelectron. 17 (2002) 541.
[33] D. Shan, Y. Y. He, S. X. Wang, H. G. Xue, and H. Zheng, Anal. Biochem. 356 (2006) 215.
[34] R. P. Liang, H. Z. Peng, and J. D. Qiu, J. Colloid Interface Sci. 320 (2008) 125.
[35] W. Y. Cai, L. D. Feng, S. H. Liu, and J. J. Zhu, Adv. Funct. Mater. 18 (2008) 3127.
[36] Y. F. Wu, C. L. Chen, and S. Q. Liu, Anal. Chem. 81 (2009) 1600.
[37] G. F. Jie, B. Liu, H. C. Pan, J. J. Zhu, and H. Y. Chen, Anal. Chem. 79 (2007) 5574.
[38] C. Hao, L. Ding, X. J. Zhang, and H. X. Ju, Anal. Chem. 79 (2007) 4442.
[39] B. Wang, J. J. Zhang, Z. Y. Pan, X. Q. Tao, and H. S. Wang, Biosen. Bioelectron. 24 (2009) 1141.
[40] Q. Xu, C. Mao, N. N. Liu, J. J. Zhu, and J. Sheng, Biosens. Bioelectron. 22 (2006) 768.
[41] J. Li and S. Dong, J. Electroanal. Chem. 431 (1997) 19.
[42] X. Chen, C. Ruan, J. Kong, and J. Deng, Anal. Chim. Acta 412 (2000) 89.
[43] B. X. Gu, C. X. Xu, and G. P. Zhu, S. Q. Liu, L. Y. Chen, M. L. Wang, J. J. Zhu, J. Phys. Chem. B 113 (2009) 6553.
[44] E. Laviron, J. Electroanal. Chem. 101 (1979) 19.
[45] R. Andreu, E. E. Ferapontova, L. Gorton, and J. J. Calvente, J. Phys. Chem. B 111 (2007) 469.
[46] X. Xu, S. Liu, and H. Ju, Sensors 3 (2003) 350.
[47] X. Liu, Y. Huang, L. Shang, X. Wang, H. Xiao, and G. Li, Bioelectrochemistry 68 (2006) 98.
[48] C. Xiang, Y. Zou, L. Sun, and F. Xu, Sens. Actuators B 136 (2009) 158.
[49] R. A. Kamin and G. S. Wilson, Anal. Chem. 52 (1980) 1198.
[50] J. Li, L. Liu, F. Xian, Z. Gui, R. Yan, F. Zhao, L. Hu, and B. Zeng, J. Electroanal. Chem. 613 (2008) 51.
[51] R. Z. Harris, P. A. Liddell, K. M. Smith, and P. R. O. D. Montellano, Biochemistry 32, (1993) 3658.